Breast tumor classification using axial shear strain elastography: A feasibility study

5 authors, including:

Arun K Thittai
Indian Institute of Technology Madras
80 PUBLICATIONS   **948** CITATIONS

SEE PROFILE

Brian Garra
Washington DC VA Medical Center
216 PUBLICATIONS   **8,846** CITATIONS

SEE PROFILE

Some of the authors of this publication are also working on these related projects:

Project   Elastography: System Performance Evaluation View project

Project   Seed point selection View project

Breast tumor classification using axial shear strain elastography: a feasibility study

Arun Thitaikumar[1,3], Louise M Mobbs[2], Christina M Kraemer-Chant[2], Brian S Garra[2] and Jonathan Ophir[1]

[1] Department of Diagnostic and Interventional Imaging, Ultrasonics Laboratory, The University of Texas Medical School, 6431 Fannin St, Houston, TX 77030, USA
[2] Department of Radiology, University of Vermont college of Medicine, Burlington, VT, USA

E-mail: Jonathan.Ophir@uth.tmc.edu

Abstract

Recently, the feasibility of visualizing the characteristics of bonding at an inclusion-background boundary using axial-shear strain elastography was demonstrated. In this paper, we report a feasibility study on the utility of the axial-shear strain elastograms in the classification of *in vivo* breast tumor as being benign or malignant. The study was performed using data sets obtained from 15 benign and 15 malignant cases that were biopsy proven. A total of three independent observers were trained, and their services were utilized for the study. A total of 9 cases were used as training set and the remaining cases were used as testing set. The feature from the axial-shear strain elastogram, namely, the area of the axial-shear region, was extracted by the observers. The observers also outlined the tumor area on the corresponding sonogram, which was used to normalize the area of the axial-shear strain region. There are several observations that can be drawn from the results. First, the result indicates that the observers consistently (∼82% of the cases) noticed the characteristic pattern of the axial-shear strain distribution data as predicted in the previous simulation studies, i.e. alternating regions of positive and negative axial-shear strain values around the tumor–background interface. Second, the analysis of the result suggests that in approximately 57% of the cases in which the observers did not visualize tumor in the sonogram, the elastograms helped them to locate the tumor. Finally, the analysis of the result suggests that for the discriminant feature value of 0.46, the number of unnecessary biopsies could be reduced by 56.3% without compromising on sensitivity and on negative predictive value (NPV). Based on the results in this study, feature values greater than 0.75 appear to be indicative of malignancy, while values less than 0.46 to be indicative of

[3] Present address: University of Texas-M.D. Anderson Cancer Center, Houston, TX, USA.

benignity. Feature values between 0.46 and 0.75 may result in an overlap between benign and malignant cases.

(Some figures in this article are in colour only in the electronic version)

Introduction

The most common cancer among women in western countries is breast cancer (Parkin *et al* 2002). In the United States, a woman's lifetime risk of developing breast cancer is 13.2%, or more than one in eight (American Cancer Society Report 2005). Recent reports demonstrate that the majority (55–68%) of breast cancer cases continue to present with palpable masses, despite the widespread use of screening mammography (Seltzer 1992, Reeves *et al* 1995). While the approach to a solid palpable breast mass is often a surgical biopsy, the malignant/benign breast biopsy ratio in the United States averages only about 1:4 (Seltzer 1992, 1997). Thus the number of unnecessary benign biopsies that are performed annually approaches 1 million. Using an average reimbursement for an open breast biopsy of $2400 (Burkhardt and Sunshine 1999), the financial cost of benign breast biopsies to the healthcare system is on the order of $2 billion annually.

Recently, Sehgal *et al* (2004) gave a summary of the role of sonography in the differentiation between malignant and benign breast lesions. When a solid lesion is present in the breast, it is not straightforward to unequivocally classify it as benign or malignant using sonography (Baker *et al* 1999, Rahbar *et al* 1999). Several approaches have been proposed to improve the accuracy of this differentiation. Stavros *et al* (1995) identified 18 sonographic features that had a high predictive value (positive or negative) and high specificity for classifying benign and malignant breast masses. These features were based on qualitative descriptions of the shape, contour, margin and ultrasonic echogenicity of the lesions. However, inter-observer variability has been a concerning issue in the characterization of solid breast masses on sonography (Mainiero *et al* 2005). These findings on inter-observer variability have been extended by several investigators (Baker *et al* 1999, Rahbar *et al* 1999). The lack of uniformity and consensus among observers' use and interpretation of various descriptive or qualitative terms that define features of malignant and benign masses often results in inconsistent diagnosis. A standardized lexicon for breast sonography was developed in 2003 by the American College of Radiology (ACR) in light of the increasing use of sonography in the classification of breast disease. Rahbar *et al* (1999) confirmed that certain sonographic features can help differentiate benign from malignant masses. However, because of inter-observer variability, they concluded that these features should not be generally applied to defer a biopsy until additional investigations in a variety of practices are undertaken. Therefore, although sonography has shown significant promise in being able to reduce the number of biopsies for solid benign masses (Taylor *et al* 2002), the practice of deferring a biopsy of solid masses on the basis of the sonographic appearance alone has not been widely adopted (Baker and Soo 2000).

Elastography is an imaging technique that applies a quasi-static compression to detect stiffness variations within ultrasonically scanned tissues. If certain tissue regions have different stiffness than others, the level of strain in those regions will generally be higher or lower than those in the surrounding material; a stiffer tissue region will generally experience less strain than a softer one. The theoretical and practical basis for elastography is given in Ophir *et al* (1999). Elastography has been shown to be helpful in detecting tumors in breast and prostate

tissues (Garra *et al* 1997, Hiltawski *et al* 2001, Lorenz *et al* 1999), in monitoring HIFU therapy in the prostate (Souchon *et al* 2003), monitoring thermal ablation (Bharat *et al* 2005, Souchon *et al* 2005), intravascular plaque characterization (de Korte *et al* 2000) and detecting and classifying thyroid tumors (Lyshchik *et al* 2005, Bae *et al* 2007) among others. The utility of elastography for the reduction of the rate of unnecessary breast biopsies has recently been demonstrated by Regner *et al* (2006), Svensson *et al* (2005) and Barr (2006). It was noted by Garra (2006) that the performance of ultrasound tumor classification is expected to improve if additional independent features become available. We anticipate that the recently developed axial-shear strain elastographic methodology (Thitaikumar *et al* 2007) may aid in breast tumor differentiation by adding independent tissue mechanics information on the bonding of a tumor to its surrounding (Fry 1954, Chen *et al* 1995, Garra *et al* 1997, Bamber *et al* 1988, Ueno *et al* 1988). Note that the lateral derivative of the axial displacements is referred to as the axial-shear strain (first term in equation (1)) (Timoshenko and Goodier 1970, Thitaikumar *et al* 2007):

$$\varepsilon_{x,y} = \left(\frac{\partial v}{\partial x} + \frac{\partial u}{\partial y} \right). \tag{1}$$

There are known observed differences in the way benign tumors and malignant tumors of the breast are bonded to their surrounding tissue, and there is currently no available modality that images this boundary bonding property directly. We demonstrated recently (Thitaikumar *et al* 2007) that the patterns of axial-shear strain distributions around inclusions are directly influenced by the bonding at the inclusion-background boundary using simulations, gelatin-phantom experiments and breast disease *in vivo*. Therefore, we hypothesize that axial-shear strain elastograms (ASSE) contain novel and independent features that may be useful for the noninvasive classification of breast tumors as benign or malignant. This hypothesis was tested in a limited retrospective *in vivo* study of pathologically confirmed benign and malignant breast lesions reported in this paper.

Materials and methods

The elucidation of the relationship between the bonding at an inclusion-background boundary and the distribution of axial-shear strain patterns around an inclusion boundary was reported in a recent manuscript (Thitaikumar *et al* 2007). However, in the practical translation of this technology to breast tumor classification, it may become clinically important to make a much simpler binary choice between loosely bonded (presumed benign) and firmly bonded (presumed malignant) tumors (Fry 1954, Chen *et al* 1995, Garra *et al* 1997, Bamber *et al* 1988, Ueno *et al* 1988). Therefore, the goal of this work was to utilize images and measurements from *in vivo* breast tumor data to demonstrate whether axial-shear strain elastograms may have a potential clinical role in the classification of breast tumors into benign and malignant categories. This study involved trained observers (discussed later in this section) for feature extraction.

In vivo data

For this study, we used previously acquired and well-controlled *in vivo* digital RF-data of breast tumors. The data were acquired by our collaborator Dr Brian Garra (University of Vermont) using a Philips HDI-1000 ultrasound scanner. The setup also consisted of a precision compression system built in our lab with previous support from P01-CA64597-10. The acquisition protocol involved multi-compression with step sizes of 0.25%. The total

compression was 5% and thus each elastogram shown in this paper is a multi-compression average of 20 realizations. A total of 115 cases have been acquired. For each case, a minimum of six acquisitions under computer-controlled compression using the transducer mounted in the frame (three each in two orthogonal planes) were acquired. Thus, we had the option to select scan data from more than one scan plane per case. For the purpose of this feasibility study, we utilized 15 benign and 15 malignant data from the database of 115 cases. The data were selected randomly.

Axial-shear strain elastogram generation

The pre-compression and temporally stretched post-compression RF signals were segmented and used in an adaptive strain estimation algorithm with lateral correction to estimate the axial displacement (Srinivasan *et al* 2002a). The displacement estimates were median-filtered with a kernel size of 3×3. This was done to increase the signal-to-noise ratio (SNR) of the elastograms obtained from the displacement estimates. A cross-correlation window length of 2 mm and a shift of 20% of the window length were used unless otherwise stated. From the estimated displacements, the axial-shear strain was estimated by extending the staggered strain estimation proposed by Srinivasan *et al* (2002b) to the lateral direction (Thitaikumar *et al* 2007). We processed all the scan data to obtain axial-shear strain elastograms and corresponding images of the local correlation coefficients. It has been shown that the correlation coefficient is indicative of the quality of the elastograms (Varghese and Ophir 1997, Céspedes *et al* 1995). Therefore, the scan having the highest mean correlation coefficient was regarded as the scan that produced the best quality image and was chosen for the study, and other scans were archived for future studies.

Features and their normalization

Based on the simulation work and preliminary *in vivo* results reported in Thitaikumar *et al* (2007), 'proximity' of the region of axial-shear strain to the lesion boundary in the sonogram and the 'normalized area of the axial-shear strain region' appear to be two of those potential features from axial-shear strain elastograms that may be able to classify a tumor as benign or malignant. An example that illustrates these features is shown in figure 1. Note that the 'proximity' parameter may relate in part to the size (i.e. area) discrepancy between the standard elastographic and sonographic appearance of breast malignancies that has been described in multiple reports in the literature of the last decade (Ophir *et al* 1996, Garra *et al* 1997, Hall *et al* 2003, Svensson *et al* 2005, Barr *et al* 2006). In fact, size discrepancy between sonographic and elastographic lesion appearance and inclusion-background strain contrast are some of the common features from the axial strain elastogram that have been and continue to be investigated by these researchers for their usefulness in the classification of breast tumors as benign or malignant. Therefore, features from axial-shear strain elastograms may ultimately be included in an expanded feature set that includes features from concurrently acquired sonograms and axial strain elastograms and used for classification of breast tumors. The use of multiple independent features (Duda *et al* 2000) is known to increase the accuracy of the classification. However, in this feasibility study, we investigate the only independent feature from the axial-shear strain elastogram, 'normalized area of axial-shear strain region', in the classification of breast tumor as benign or malignant.

It was shown in our previous report (Thitaikumar *et al* 2007) that the area of the axial-shear strain region must be normalized for the area of the tumor, applied axial compressive strain and tumor–background modulus contrast. As noted in the literature, there exists a size
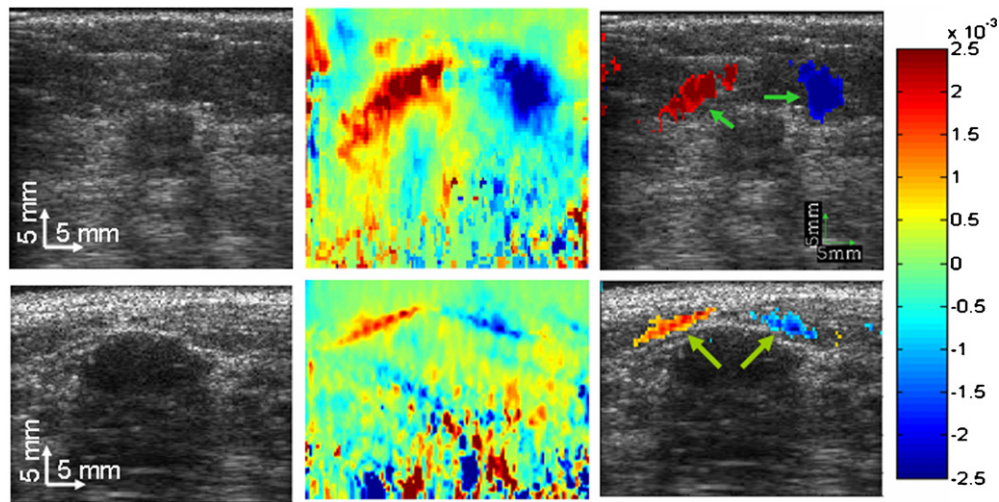
Figure 1. Sonogram (first column), axial-shear strain elastogram (second column) and composite image obtained by superimposing the axial-shear strain elastogram on top of the sonogram (third column) of a cancer (top row) and benign lesion (bottom row) are shown. Only the pixels whose shear strain value and corresponding correlation coefficient were greater than 0.125% and 0.75 respectively were made visible in the composite image. The applied axial compression strain was 0.25%. Axial-shear strain regions are pointed by the green arrow in the composite image.

difference between tumor appearance in sonograms and elastograms for the case malignant tumors. Therefore, in order to normalize the features for the size of the lesion, one could estimate the lesion size from either the sonogram or the corresponding axial elastogram. In this study, we have normalized the features using the size as measured from the sonogram.

It may appear that the normalization for applied axial strain can be done in a similar fashion to that which was reported in previous study (Thitaikumar *et al* 2007), i.e. contour thresholds for segmenting the axial-shear strain region may be set as a percentage of the known applied axial strain. However, the axial-shear strain values are influenced by the elastic modulus contrast as well. The normalization for elastic modulus contrast is important and also needs to be done by adjusting the contour threshold. However, the elastic modulus contrast is not known *a priori*. In order to overcome this difficulty, we decided to let the observer manually outline the axial-shear strain region. Later, statistics of the pixel values were used to refine and obtain the normalized area of the axial-shear strain region. The statistics in this case involved the mean of the axial-shear strain values within the region outlined by the observer. This method can be considered a self-normalizing technique where the contour threshold is set as a percentage (70%) of the mean value, which will normalize the axial-shear strain features for the applied axial strain and elastic modulus contrast simultaneously.

Observer training

We engaged *three* observers in this study. Observers 1 and 2 were trained sonographers while observer 3 was not. However, observer 3 was a scientist who was very familiar with axial-shear strain elastograms. Observer 1 had never been exposed to axial-shear strain elastograms while observer 2 had some familiarity. These observers were trained in two areas. First, the observers were presented with sample images of axial-shear strain elastograms of benign and malignant tumors. An example set of training images are shown in figure 2. During this
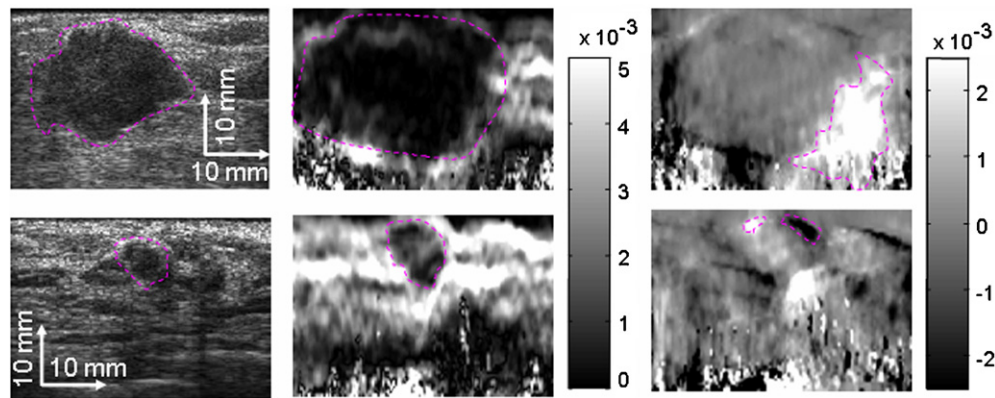
Figure 2. An example of the images used during *observer training*. Sonograms (first column), axial elastograms (second column) and ASSEs (third column) of a cancer (top row) and benign lesion (bottom row) are shown. The applied axial compression strain was 0.25%. Observer's outline (–) of the tumor appearance in sonograms and elastograms is shown. In addition, the observer's outline of the feature in ASSE is also shown.

phase, the observers were given handouts (see appendix A) containing a description of the new modality and instructions on what the regions of interest in these images are. Second, the observers were trained to use a Matlab®-based GUI (graphical user interface) software to select the region of interest. We used four benign and five malignant tumor cases for observer training purpose, and the observers were able to compare his/her assessment with the pathology reports. Once trained, the observers were presented with the testing data set in random order, which comprised 11 benign and 10 malignant tumor cases. The observers were blinded to the results from pathology of the testing data set. The primary author facilitated the observer training and did not participate as an observer.

Image evaluation protocol

The feature from the axial-shear strain images and tumor appearance in sonograms and axial elastograms were outlined by the trained observers using the interactive GUI software routine. The sequence of steps is illustrated in the form of a flowchart in figure 3. The software randomly selected a case from the testing set and displayed the full set of images, axial strain elastograms, ASSE and sonogram. By making the case selection random, we aimed to keep the observer performance unbiased. The GUI allowed the observer to outline the sonographic and elastographic lesion with the mouse after visual inspection. The number of pixels within this outline was used to automatically compute the size (area) of the tumor as visualized in these two images. One of the major limitations in observer-based feature extraction in sonography is due to inter-observer variability (Sehgal *et al* 2004). In an attempt to reduce this variability, Sehgal *et al* (2004) suggested the use of computer-based feature extraction. For the same reason, we computed the features from the axial-shear strain elastogram in a semi-automated manner. We allowed the observer to manually outline the gross region of interest for the feature and used the statistics of the pixel values within the outlined region to automatically compute the feature values. The automation of the quantification is aimed to improve the objectivity of the measurements while observer outlining excludes regions that are irrelevant to the tumor boundary that might otherwise corrupt the measurements. The observers' outline of the sonographic lesion was used for the inclusion-size normalization. Note that for the
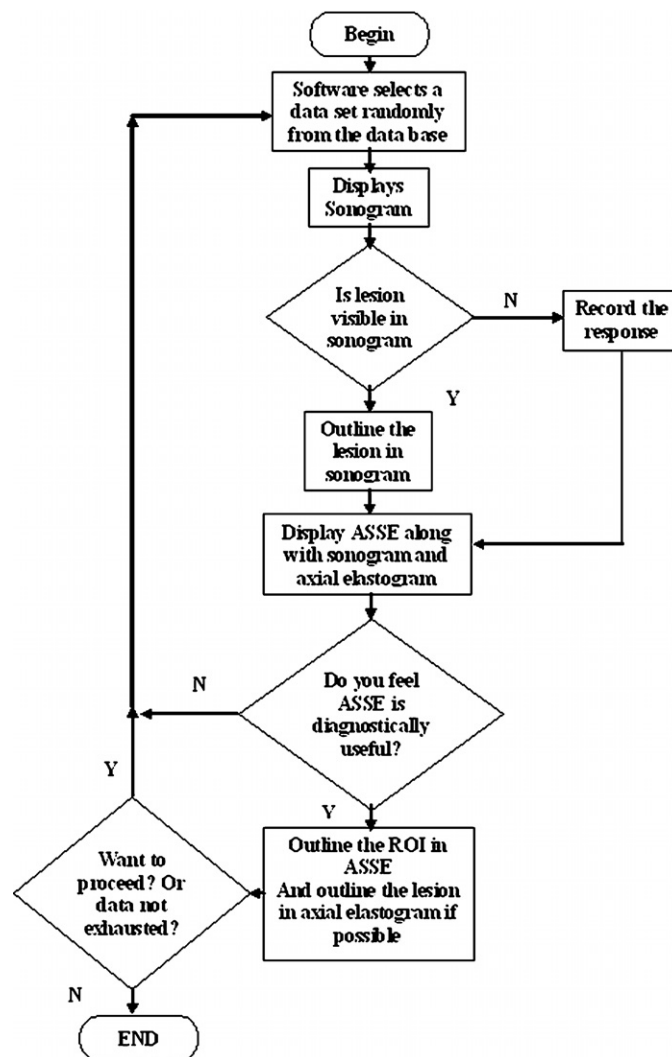
Figure 3. Flowchart describing the image evaluation protocol.

purposes of this study we utilized only those data for which the observer determines that the lesion is visible in the sonogram. It must be noted that all the images were displayed using standard grayscale. This may not be surprising for sonogram and axial elastogram. But, the axial-shear strain elastograms that have been reported previously by our group were in color (Thitaikumar *et al* 2007, Thitaikumar and Ophir 2006). However, this was only done when ASSEs were superimposed on the corresponding sonograms.

Results

Twenty-one data sets were presented to the observers for feature extraction (11 B = benign and 10 M = malignant). Details on the number of cases for which feature extraction from sonogram and/or ASSE was done by each observer is reported in table 1.

Table 1. The number of cases for which feature was extracted from sonogram and/or ASSE.

(A) Observer number	Number of cases for which a tumor was outlined on the sonogram by the observer		Number of cases for which the ROI was outlined in ASSE by the observer	
	(B) Blinded to elastograms	(C) Not blinded to elastograms	(D) Had a tumor outlined in the sonogram	(E) Did not have tumor outlined in the sonogram
1	13	5	14	1
2	12	4	15	5
3	18	2	17	0

Table 2. The number of benign (B) and malignant (M) cases for which features from the sonogram and the ASSE were extracted.

Observer 1	8-B, 6-M
Observer 2	8-B, 7-M
Observer 3	9-B, 8-M

Table 3. Percentage of cases in which the elastograms helped the observer to visualize the tumor in the sonogram.

Observer 1	$5/8 \sim 62\%$
Observer 2	$4/9 \sim 44\%$
Observer 3	$2/3 \sim 66\%$

It is clear from the last column in table 1 that there were few cases in which the observer chose to outline an ROI in ASSE while not outlining the tumor in the corresponding sonogram. Also note that on the average the observers were able to outline an ROI in ASSE in approximately 82% of the cases. However, for the purpose of computing the feature from ASSE, 'normalized area of the axial-shear strain region', we require that the tumor outline on the sonogram and the ROI outline on the ASSE are present simultaneously. The number of benign and malignant cases for which these two were outlined, by each of the observer, is shown in table 2.

An important aspect that needs further attention is the number of cases reported in column C of table 1. This column reports the number of cases for which the observers outlined a tumor on the sonogram, only after looking at the corresponding elastograms (axial elastograms and ASSE). In other words, these are the cases in which the access to elastograms helped in visualizing a tumor in the sonogram, which was otherwise not apparent to the observer. This is reported in terms of percentage in table 3. The importance of this number is further detailed in the discussion section.

Summary of the performance by the observer

Figure 4 shows a plot of the normalized area of the values of the axial-shear strain region feature obtained by each observer for benign and malignant cases. It is clear from the plots that there is a tendency for the malignant cases to cluster toward larger normalized feature values compared to the benign cases for all the observers. This is consistent with the results
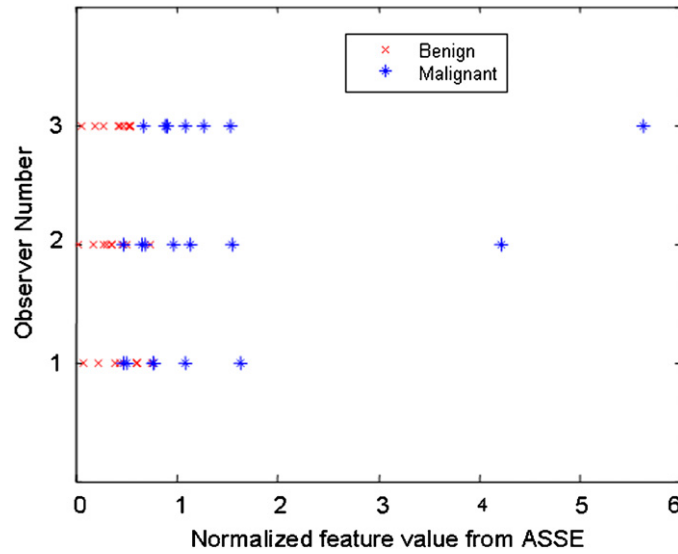
Figure 4. Plot of the normalized values of the area of the axial-shear strain region feature from ASSE as obtained by each of the observers. Note that the malignant cases tend to cluster toward larger feature values compared to the benign cases, as determined by all the observers.

reported in Thitaikumar *et al* (2007) based on simulation work. However, the classification results will depend on the selected feature threshold value (discriminant value). In order to analyze the classification performance by the observers we will use the metrics described below.

	Condition (as determined by 'pathology')			
	Malignant (*true*)	Benign (*false*)		
Test Outcome				
Positive	True positive (TP)	False positive (FP)	→	Positive predictive value (PPV)
Negative	False negative (FN)	True negative (TN)	→	Negative predictive value (NPV)
	↓	↓		
	Sensitivity	Specificity		

$$\text{Sensitivity} = \frac{\text{TP}}{(\text{TP} + \text{FN})}, \qquad \text{Specificity} = \frac{\text{TN}}{(\text{FP} + \text{TN})},$$

$$\text{PPV} = \frac{TP}{(\text{TP} + \text{FP})} \quad \text{and} \quad \text{NPV} = \frac{\text{TN}}{(\text{TN} + \text{FN})}.$$

In any classification problem, the most desirable result is to have 100% sensitivity and 100% specificity (Duda *et al* 2000); however, this is rarely achieved. Depending on the particular classification problem, one or the other values are traded off. The authors understand that the features from ASSE will not be a stand-alone feature for classification, but rather may supplement the existing feature set from sonograms and axial elastograms. The ultimate importance of the feature from ASSE is to aid in reducing the number of unnecessary biopsies. Therefore, in the problem of tumor classification using ASSE we analyzed

Table 4. Discriminant value for each observer that yielded the best NPV.

Observer 1[a] ($\mu = 0.46$)	Malignant	Benign
Positive	6	4
Negative	0	4

Observer 2[b] ($\mu = 0.46$)	Malignant	Benign
Positive	7	2
Negative	0	6

Observer 3[c] ($\mu = 0.55$)	Malignant	Benign
Positive	8	0
Negative	0	9

[a] NPV and sensitivity = 100%, specificity = 50%.
[b] NPV and sensitivity = 100%, specificity = 75%.
[c] NPV and sensitivity = 100%, specificity = 100%

Table 5. Performance of observer 3 at a discriminant value that yielded the best performance for observers 1 and 2.

Observer 3 ($\mu = 0.46$)	Malignant	Benign
Positive	8	5
Negative	0	4

NPV and Sensitivity = 100%, Specificity = 44%

sensitivity, specificity and NPV, favoring higher values for NPV and sensitivity compromising specificity. This is because we cannot afford to misclassify any malignant tumors (determined by sensitivity) and at the same time, it is important to correctly classify a benign tumor (as determined by NPV).

For each observer, the discriminant threshold value (μ) that yielded the best NPV is reported in table 4.

From the above analysis it is clear that the discriminant value that yields best NPV and specificity for observer 3 is slightly different from the other two observers. It is not surprising that there is a small inter-observer variability. If we use the same discriminant value as of observers 1 and 2 for observer 3, note that the specificity decreases (see table 5). However, the analysis of the results suggests that the average performance of the observers (for the same discriminant value, $\mu = 0.46$) results in a specificity of 56.3% and sensitivity and NPV of 100%. This result implies that without compromising on sensitivity and NPV we might be able to reduce the number of unnecessary biopsies by 56.3%.

Discussion

In our recent publication (Thitaikumar *et al* 2007) feasibility to produce ASSE *in vivo* was demonstrated. It was shown that the bonding at the inclusion-background boundary influenced the axial-shear strain distribution pattern. In the study reported in this paper, we performed an initial feasibility study on the ability of a feature from ASSE to classify breast tumor as benign or malignant. The analyses of the results portray several interesting aspects. Firstly, note that in approximately 82% (average among the three observers) of the cases presented, the observers noticed the expected characteristic axial-shear strain pattern and hence outlined the ROI. This is very promising because the data were acquired for a previous study and were not
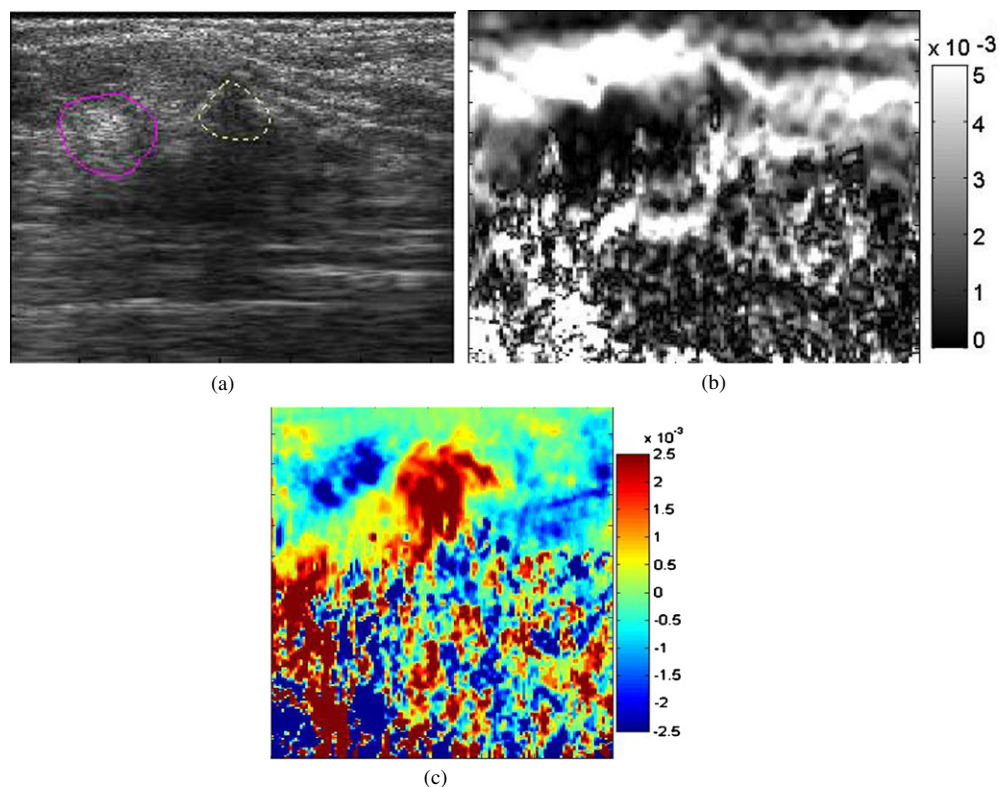
Figure 5. An example that demonstrates the ability of the axial-shear strain elastogram (right), to help locate the lesion in the sonogram (left), along with the axial strain elastogram (center). One observer's outline of a perceived tumor in the sonogram by looking at the sonogram alone (- - - -) and in conjunction with elastograms (– – – magenta) is also shown.

optimized for ASSE. Therefore, there is latitude to improve the consistent appearance of the characteristic axial-shear strain distribution pattern. Secondly, on average (among the three observers, table 3) there is 57.3% improvement in the number of cases where the elastograms (either axial elastogram or ASSE) helped visualize the tumor in the sonogram. Even though the task was not to compare elastograms against sonograms, we felt that it is important to report this result because it may merit further investigation. For example, Figure 5 shows a scan that demonstrates that looking at axial-shear strain elastograms and axial elastograms helps in visualizing lesions in the sonogram that otherwise would have been wrongly identified or missed. Observe how having the axial-shear strain elastogram helps in clearly demarcating the lesion margins in the sonogram. In this example, looking at only the sonogram the observer outlined the tumor as shown by dotted lines, whereas, after looking at the elastograms the observer re-outlined the tumor as shown by the solid line (figure 5(a)). Looking at this example, the observer commented that the axial-shear strain elastograms helped in better defining the proximal tumor boundary and thus may improve the accuracy of needle biopsy sampling. Of course, these are issues that need further investigation and to be repeated on a larger data set.

Clearly, an important factor that determines the classification performance is the discriminant value. Based on the result in this study, feature values greater than 0.75 appear to be indicative of malignancy, while values less than 0.46 to be indicative of benignity. The

feature value in between 0.45 and 0.75 may result in the overlap of benign and malignant cases. It must be pointed out that only three observers were involved in the study and the threshold values are from a small number of data sets. Please note that the thresholds will become more stable as the data set grows and move board-certified sonographers are utilized for the study. It must be noted that the thresholds will become more stable as the data set grows and more board-certified sonographers are utilized for the study. Nevertheless, the plot shown in figure 4 for benign and malignant cases from the three observers is encouraging. It is apparent from figure 4 that the normalized axial-shear strain region feature from ASSE has a tendency to cluster at higher values for malignant cases compared to benign cases. Another important aspect that will influence classification performance using ASSE has to do with observer training. It can be noted that the performance of observer 3 (highly trained) was different from observer 1 (trained for the first time). Observer 3 had outlined features on 17 cases compared to 14 cases by observer 1, indicating the level of confidence in identifying the ROI. Also, the separation between benign and malignant for observer 3 is superior (no overlap) compared to observer 1. Even though the numbers on the NPV, sensitivity and specificity are encouraging, the result must be seen only as a demonstration of the ability of feature from ASSE to aid in reducing the number of unnecessary biopsies.

Conclusion

In this paper, we have shown that the feature from the axial-shear strain elastogram, 'the normalized area of the axial-shear strain region' (as identified in Thitaikumar *et al* (2007)), has the potential to aid in breast tumor classification, and thus to reduce the number of unnecessary true benign biopsies. The results from this study, which had a limited data set and only three observes, bode well for the continued investigation of the applicability of ASSE to breast tumor classification.

Acknowledgments

Appendix A. A brief description of the axial-shear strain modality

An axial-shear strain elastogram (ASSE) is an image that maps the local axial-shear strain experienced by the tissue elements in response to quasi-static external axial compression. Unlike a sonogram, the region of interest (ROI) in an ASSE is not the lesion itself, but rather a region near the lesion boundary. The sign of the shear strain values can be either positive or negative depending on the directionality within the coordinate system used to display the image. Since the ROI in the ASSE does not usually overlap with the sonographic lesion, the ASSE may be superimposed on the corresponding sonogram to form a composite image, which visualizes the ROI in ASSE in the context of the sonographic lesion. The task of the observer is to outline the ROI from the ASSE that is likely due to the tumor visible in the sonogram. Note that in most *in vivo* sonograms the echo signals distal to the tumor have a poor signal-to-noise ratio due to attenuation and shadowing effects. Consequently, we are not able to produce reliable images of shear strains in these distal regions with current algorithms. Therefore, in most cases the observer may see shear strain region only near the proximal lesion boundary.

Table 6. Image acquisition details and tumor classification from histopathology.

ELASTO case no	Histopathology classification	Scanner depth (mm)	Breast thickness (mm)	1% Pre-compression depth (mm)	Acquisition orientation
V0074	Fibroadenoma	28	26	0.26	R
V0078	Fibroadenoma	37	35	0.35	R
V0083	Fibroadenoma	45	41	0.41	R
V0091	Invasive ductal adenocarcinoma, nuclear grade 2, moderate differentiation. DCIS, solid pattern nuclear grade 2–nuclear grade 2, DCIS nuclear grade 2	37	30	0.3	R
V0092	Invasive ductal adenocarcinoma, Synchronous tumors, nuclear grade 2, well differentiated. DCIS cribriform and solid Patterns, nuclear grade 2	45	35	0.35	R
V0094	Fibroadenoma	37	35	0.35	R
V0130	Invasive lobular with synchronous invasive ductal adenocarcinoma, nuclear grade 2, well differentiation of both tumors	37	28	0.28	A
V0131	Invasive lobular adenocarcinoma, nuclear grade 2, well differentiation, lymphovascular invasion present	45	43	0.43	A
V0156	Adenocarcinoma,invasive ductal nuclear grade 2, moderate differentiation, DCIS, solid pattern, LCIS	56	52	0.52	A
V0163	Fibroadenoma	45	48	0.48	A
V0171	Fibroadenoma	45	46	0.46	R
V0179	Invasive lobular adenocarcinoma (two primaries in the lower inner quadrant) moderate differentiation, nuclear grade 2, extensive lymphovascular invasion, with prominent signet ring cells	56	50	0.5	AR
V0185	DCIS, cribiform type, nuclear grades 2 and 3, intraductal papilloma, fibrocystic changes, sclerosing adenosis, microcyst formation, apocrine metaplasia, interlobular fibrosis No invasive carcinoma present	45	39	0.39	AR
V0190	Hyalinized fibroadenoma	28	28	0.28	AR
V0191	Nodular fibrocystic changes, focal moderate ductal eppithelial hyperplasia, microcyst formation, apocrine metaplasia, adenosis, cellular interlobular fibrosis	28	20	0.2	AR
V0193	Adenocarcinoma, invasive ductal, nuclear grades 1 and 2, well-differentiated. focal DCIS, cribriform pattern, with focal necrosis neclear grade 1	45	38	0.38	AR
V0195	Adenocarcinoma, invasive ductal type, moderately differentiated, nuclear grade 2, fibrocystic changes, interlobular fibrosis, microcalcifications associated with benign tissue	28	20	0.2	AR
V0196	Adenocarcinoma, invasive lobular, moderately differentiated. Multifocal lesion, pleomorphic lobular carcinoma in situ is present. Atypical ductal hyperplasia, nuclear grade 2	37	35	0.35	R
V0202	Fibroadenoma with myxoid stroma	28	24	0.24	R
V0203	Hyalinized fibroadenoma	37	40	0.4	R
V0213	Fibroadenoma, focal microcalcifications associated with benign breast tissue	45	38	0.38	AR

The following is a guideline for the observer while outlining the axial-shear strain ROI.

Step 1: Do you think the current axial-shear strain elastogram and corresponding sonogram is 'gradable'?

Step 2: Select a small region from ASSE that you think is the axial-shear strain region corresponding to the known sonographic lesion.

Step 3: Outline the lesion from Sonogram.

Step 4: Enter the number of quadrants of the tumor boundary that you feel captures the 'clean' shear strain region

- Choose only a maximum of two quadrants.
- Unless there is a compelling reason, identify the shear strain region only from first and second quadrants as often as possible.
- Restrict the outlining of shear strain regions to around the sonographically identified lesion.
- If there are a few missing pixels that lead to ambiguity of whether it is *one* larger contour with missing pixels or *multiple* small contours, use your judgment. In most cases we are looking for only one contour per quadrant!

Step 5: Outline the lesion from the axial elastogram. If you do not visualize the complete lesion, please use your judgment from the corresponding sonogram to complete the lesion or do not grade it at all. Whatever you decide at the beginning should be consistent throughout.

Step 4: If there is any problem/questions during the exercise, please do not continue without further assistance.

Appendix B. Details on the tumor data that were used in the study

Details regarding tumor type, its location and acquisition position are listed in table 6.

References

American Cancer Society 2005 *Breast Cancer Facts & Figures 2005–2006* (Atlanta: American Cancer Society, Inc.)

American College of Radiology (ACR) 1998 *Illustrated Breast Imaging Reporting and Data System (BI-RADSTM)* 3rd edn (Reston, VA: American College of Radiology)

Bae U, Dighe M, Dubinsky T, Minoshima S, Shamdasani V and Kim Y 2007 Ultrasound thyroid elastography using carotid artery pulsation: preliminary study *J. Ultrasound. Med.* **26** 797–805

Baker J A, Kornguth P J, Soo M S, Walsh R and Mengoni P 1999 Sonography of solid breast lesions observer variability of lesion description and assessment *Am. J. Roentgenol.* **172** 1621–5

Baker J A and Soo M S 2000 The evolving role of sonography in evaluating solid breast masses *Semin. Ultrasound CT MR* **21** 286–96

Bamber J C, De Gonzale L, Cosgrove D A, Simmons P, Davey J and McKinna J A 1988 Quantitative evaluation of real-time ultrasound features of the breast *Ultrasound Med. Biol.* **14** 81–7

Barr R G 2006 Clinical applications of a real time elastography technique in breast imaging *Proc. 5th Int. Conf. Ultrasonic Measurement and Imaging of Tissue Elasticity* p 112

Bharat S, Techavipoo U, Kiss M, Liu W and Varghese T 2005 Monitoring stiffness changes in lesions after radiofrequency ablation at different temperatures and durations of ablation *Ultrasound Med. Biol.* **31** 415–22

Burkhardt J H and Sunshine J H 1999 Core-needle and surgical breast biopsy: comparison of three methods of assessing cost *Radiology* **212** 181–8

Céspedes I, Huang Y, Ophir J and Spratt S 1995 Methods for estimation of subsample time delays of digitized echo signals *Ultrason. Imaging* **17** 142–71

Chen E J *et al* 1995 Ultrasound tissue displacement imaging with application to breast cancer *Ultrasound Med. Biol.* **21** 1153–62

de Korte C, Pasterkamp G, van der Steen A F W, Woutman H A and Bom N 2000 Characterization of plaque components with intravascular ultrasound elastography in human femoral and coronary arteries *in vitro Circulation* **102** 617–23

Duda R O, Hart P E and Stork D G 2000 *Pattern Classification* 2nd edn (New York: Wiley)

Fry K E 1954 Benign lesions of the breast *CA Cancer J. Clin.* **4** 160–1

Garra B S *et al* 1997 Elastography of breast lesions: initial clinical results *Radiology* **202** 79

Garra B S, Mobbs L M, Chant C M and Ophir J 2006 Clinical breast elastography: blinded reader performance and strategies for improving reader performance *Proc. 5th Int. Conf. Tissue Elasticity (Snowbird, UT, Oct 2006)*

Hall T J, Zhu Y and Spalding C S 2003 *In vivo* real-time freehand palpation imaging *Ultrasound Med. Biol.* **29** 427–35

Hiltawski K K *et al* 2001 Freehand ultrasound elastography of breast lesions: clinical results *Ultrasound Med. Biol.* **27** 1461–9

Lorenz A *et al* 1999 A new system for the acquisition of ultrasonic multicompression strain images of the human prostate *in vivo IEEE Trans. Ultrason. Ferroelec. Freq. Cont.* **46** 1147–54

Lyshchik A *et al* 2005 Thyroid gland tumor diagnosis at US elastography *Radiology* **237** 202–11

Mainiero M B *et al* 2005 Characterization of breast masses with sonography: can biopsy of some solid masses be deferred? *J. Ultrasound Med.* **24** 161–7

Ophir J *et al* 1996 Elastography: ultrasonic imaging of tissue strain and elastic modulus *in vivo Eur. J. Ultrasound* **3** 49–70

Ophir J *et al* 1999 Elastography: ultrasonic estimation and imaging of elastic properties of tissues *Proc. Instn Mech. Eng. (UK)* **vol. 213 (H3)** 203–33

Parkin D M, Bray F, Ferlay J and Pisani P 2002 Global cancer statistics *CA Cancer J. Clin.* **55** 74–108

Rahbar G *et al* 1999 Benign versus malignant solid breast masses: US differentiation *Radiology* **213** 889–94

Reeves M *et al* 1995 Determinants of breast cancer detection among Wisconsin (United States) women, 1988–1990 *Cancer Causes Control.* **6** 103–11

Regner D M *et al* 2006 Breast lesions: evaluation with US strain imaging—clinical experience of multiple observers *Radiology* **238** 425–37

Sehgal M C, Cary W T, Kangas S A, Weinstein P S, Schultz M S, Arger H P and Conant F E 2004 Computer-based margin analysis of breast sonography for differentiating malignant and benign masses *J. Ultrasound Med.* **23** 1201–9

Seltzer M H 1992 The significance of breast complaints as correlated with age and breast cancer *Am. Surg.* **58** 413–7

Seltzer M H 1997 Preoperative prediction of open breast biopsy results *Cancer* **79** 1822–7

Souchon R, Bouchoux G, Maciejko E, Lafon C, Cathignol D, Bertrand M and Chapelon J 2005 Monitoring the formation of thermal lesions with heat-induced echo-strain imaging: a feasibility study *Ultrasound Med. Biol.* **31** 251–9

Souchon R, Rouviere O, Gelet A, Detti V, Srinivasan S, Ophir J and Chapelon J Y 2003 Visualization of HIFU lesions using elastography of the human prostate *in vivo*: preliminary results *Ultrasound Med. Biol.* **29** 1007–15

Srinivasan S *et al* 2002a Analysis of an adaptive strain estimation technique in elastography *Ultrason. Imaging* **24** 109–18

Srinivasan S, Ophir J and Alam S K 2002b Elastographic imaging using staggered strain estimates *Ultrason. Imaging* **25** 229–45

Stavros A T, Thickman D, Rapp C L, Dennis M A, Parker S H and Sisney G A 1995 Solid breast nodules: use of sonography to distinguish between benign and malignant lesions *Radiology* **196** 123–34

Svensson W E *et al* 2005 Elasticity imaging of 67 cancers and 167 benign breast lesions shows that it could halve biopsy rates of benign lesions *Proc. 4th Int. Conf. Ultrasonic Measurement and Imaging of Tissue Elasticity* p 87

Taylor K J *et al* 2002 Ultrasound as a complement to mammography and breast examination to characterize breast masses *Ultrasound Med. Biol.* **28** 19–26

Thitaikumar A, Krouskop T A, Garra B S and Ophir J 2007 Visualization of bonding at an inclusion boundary using axial-shear strain elastography: a feasibility study *Phys. Med. Biol.* **52** 2615–33

Thitaikumar A and Ophir J 2007 Effect of lesion boundary conditions on axial strain elastograms: a parametric study *Ultras. Med. Biol.* **33** 1463–7

Timoshenko S P and Goodier J N 1970 *Theory of Elasticity* (New York: McGrow-Hill) pp 8–11

Veno E, Tohno E, Soeda S, Asaoka Y, Itoh K, Bamber J C, Blaszczyk M, Davey J and McKinna J A 1988 Dynamic tests in real-time breast echography *Ultrasound Med. Biol.* **14** 53–7

Varghese T and Ophir J 1997 The nonstationary strain filter in elastography: Part I. Frequency dependent attenuation *Ultrasound Med. Biol.* **23** 1343–56